JGR Space Physics

RESEARCH ARTICLE
10.1029/2019JA027429

Key Points:
- Low-frequency magnetic field fluctuations in the topside *F* region polar ionosphere show scale-invariance
- Anomalous scaling (multifractal/intermittent) features and anisotropy of magnetic field fluctuations are studied
- A link between the scale-invariance of fluctuations and the filamentary nature of field-aligned currents is discussed

Correspondence to:
G. Consolini,
giuseppe.consolini@inaf.it

Citation:
Consolini, G., De Michelis, P., Alberti, T., Giannattasio, F., Coco, I., Tozzi, R., & Chang, T. T. S. (2020). On the multifractal features of low-frequency magnetic field fluctuations in the field-aligned current ionospheric polar regions: Swarm observations. *Journal of Geophysical Research: Space Physics*, *125*, e2019JA027429. https://doi.org/10.1029/2019JA027429

Received 18 SEP 2019
Accepted 25 MAR 2020
Accepted article online 15 APR 2020

On the Multifractal Features of Low-Frequency Magnetic Field Fluctuations in the Field-Aligned Current Ionospheric Polar Regions: Swarm Observations

G. Consolini[1], P. De Michelis[2], T. Alberti[1], F. Giannattasio[2], I. Coco[2], R. Tozzi[2], and T. T. S. Chang[3]

[1]INAF-Istituto di Astrofisica e Planetologia Spaziali, Rome, Italy, [2]Istituto Nazionale di Geofisica e Vulcanologia, Rome, Italy, [3]Kavli Institute for Astrophysics and Space Research, Massachusetts Institute of Technology, Cambridge, MA, USA

Abstract Recent findings on the nature of magnetic field fluctuations in the high-latitude ionospheric regions have suggested the existence of scaling features, which are the signature of the occurrence of turbulence. These features mainly characterize the magnetic field fluctuations in those regions where the field-aligned currents flow. Here, we investigate the nature of the Earth's magnetic field fluctuations using the high-resolution (50 Hz) magnetic measurements from the European Space Agency Earth's observation mission Swarm. Our study indicates that spatiotemporal anomalous scaling features characterize low-frequency magnetic field fluctuations in the high-latitude ionospheric regions of field-aligned currents at spatial scales in the range 0.8–80 km (timescales in the range 0.1–10 s). The signature of a multifractal nature of these fluctuations suggests a highly complex structure of the field-aligned currents. Our results support the view of inhomogeneous (filamentary) field-aligned currents, which can have relevant implications in the comprehension of the physical processes responsible for the magnetospheric-ionospheric coupling and ionospheric heating.

1. Introduction

Since the early 90s, it has been argued that several regions of the circumterrestrial space are characterized by a multiscale dynamics, which is mainly due to the occurrence of intermittent turbulent phenomena and complexity (Borovsky et al., 1997; Bruno & Carbone, 2016; Chang et al., 2003, 2004). Indeed, turbulence, which is a prevalent phenomenon in space plasmas, generates multiscale coherent structures over a wide range of spatiotemporal scales. In magnetized plasmas, these coherent structures, consisting of bundles of fluctuations, may take the shape of flux tubes, current filaments, propagating nonlinear solitary waves, convective structures, and so on, depending on the local and global magnetic field and plasma topology (Chang et al., 2004). In the near-Earth central plasma sheet of the magnetospheric tail region, the stochastic evolution and interaction of such coherent structures are suggested to be responsible for the occurrence of sporadic plasma acceleration, heating, and energization (e.g., bursty bulk flows, localized reconnections). These processes have been detected by several space missions, such as ISEE, AMPTE, and Cluster (Angelopoulos et al., 1999; Chang et al., 2003, 2004; Lui et al., 1998), and have been suggested to be responsible for the stochastic nature of auroral breakups (Lui et al., 1998). A further consequence of the dynamics of such coherent structures is the emergence of spatiotemporal intermittency in an overall turbulent plasma, that is, an inhomogeneous turbulent energy dissipation pattern.

In the framework of high-latitude ionosphere, turbulence is expected to be a relevant phenomenon in the polar regions where particle precipitation occurs (Kintner & Seyler, 1985). Indeed, in some cases, turbulence has been invoked to explain the formation of ionospheric irregularities (Booker, 1956; Dagg, 1957; Kintner & Seyler, 1985). According to Kintner and Seyler (1985), the range of scales where turbulence plays a relevant role is from few meters up to $\sim$ 1000 km in the topside *F* region of the high-latitude ionosphere, a range of spatial scales where large magnetic and electric field fluctuations have been observed. In recent years, an extensive literature has demonstrated that high-latitude magnetic and electric field fluctuations, as well as plasma density variations, show scale-invariance and intermittent turbulent features (De Michelis et al., 2015; 2017; Golovchanskaya et al., 2006, Spicher et al., 2015; Tam Sunny et al., 2005). Furthermore,

the scale-invariance nature of magnetic field fluctuations has been shown to be a function of the different polar regions (polar cap, cusp, auroral oval), the magnetic local time, the interplanetary magnetic field conditions and the geomagnetic activity disturbance level (De Michelis et al., 2015, 2017, 2019).

Different mechanisms have been proposed as possible sources of the observed turbulent fluctuations, among which the occurrence of strong shear flows and particle precipitations seem to play a relevant role. Thus, among the different high-latitude ionospheric regions (i.e., polar cap, cusp, auroral oval, etc.), those associated with the field-aligned currents (FACs) with particle precipitation enhancements during periods of high geomagnetic activity represent a good candidate for turbulence to occur. This scenario is supported by the experimental work of Pokhotelov et al. (1994) where it has been shown that a likely physical mechanism for the excitation of turbulent noise fluctuations in the ionospheric plasma can be the occurrence of localized FACs and the related current instabilities.

The FACs were originally postulated by Birkeland (Birkeland, 1908) and detected for the first time 60 years later by spacecraft observations of localized magnetic fluctuations (Cummings & Dessler, 1967; Zmuda et al., 1966). One of the first sketch of these electric currents was proposed by (Iijima et al., 1976; Iijima & Potemra, 1978) based upon the analysis of the single-polar-orbiting Triad satellite. In this sketch, the pattern of the distribution of FACs, also known as Birkeland currents, is represented by two belts of electric currents (region-1 and region-2) that flow upward and downward along the magnetic field lines according to the latitude and magnetic local time. Later, by analyzing the periods characterized by a northward interplanetary magnetic field, Iijima (1984) and Iijima and Shibaji (1987) found another stable FAC system at higher latitude than region-1, the so-called Northward B_Z FAC system. FACs are located at high latitudes in both hemispheres and flow along geomagnetic field lines connecting the Earth's magnetosphere to the ionosphere and playing an important role in energy and momentum transfer between different plasma regions: the solar wind and magnetosphere on the one hand and the ionosphere and thermosphere on the other hand. As a consequence, the knowledge of their structure and dynamics is of uppermost importance to the understanding of how the solar wind energy is transferred from the magnetosphere to the ionosphere and thermosphere and to the comprehension of those physical processes which are related to the solar wind-magnetosphere-ionosphere coupling.

In recent years, there has been an increasing amount of literature on the statistical investigation of high-latitude FACs using observations mainly from low-orbiting satellites (e.g., CHAMP, AMPERE, DMSP, and Swarm). Results have been also compared with studies on the large-scale convection topology based on ground-based magnetometer networks and coherent/incoherent auroral radars (e.g., EISCAT and SuperDARN) (Chisham et al., 2007; Sofko et al., 1995). The morphology of this current system on large spatial scales is now well established (Anderson et al., 2008; Gjerloev et al., 2011), as well as its variability with solar wind-magnetosphere coupling conditions (Anderson et al., 2005; Cheng et al., 2013; Korth et al., 2010) and its dynamics with respect to various geophysical, seasonal, and local time conditions (Christiansen et al., 2002; Papitashvili et al., 2001; Papitashvili & Rich, 2002). Although significant progresses have been achieved on this three-dimensional current flow in the auroral zone, some scientific questions remain to be answered. In this context, an interesting topic is the characterization of the FAC structure on small spatial scales. Indeed, in addition to large-scale FAC structures, which are characterized by widths from few hundreds to a thousand kilometers, some small-scale FAC structures were also observed by satellite measurements (Lühr et al., 1994; Neubert & Christiansen, 2003; Stasiewicz & Potemra, 1998). Surveys such as those conducted by Neubert and Christiansen (2003) have shown that small-scale FACs can be found throughout the auroral oval although the most intense of these are in the cusp and prenoon cusp region. These currents, with typical widths of a few hundred meters, have intensities reaching several hundreds μAm^{-2} (Lühr et al., 1994; Stasiewicz & Potemra, 1998). It has been also suggested that the small-scale FACs can have an important role in the heating of ionosphere and thermosphere. For this reason, it is not enough to consider only the FAC structures on large scales but also important to take into account the local heating resulting from FAC structures on small scales [Neubert and Christiansen, 2003], whose intensity is several orders of magnitude larger than those characterizing the FAC structures on large scales. It is expected that the heating of the ionosphere and thermosphere due to the processes related to FACs can be larger when FACs at all scales are considered. For this reason, it is important to characterize them and investigate their energy deposition at all scales in the future comprehensive models of magnetosphere-ionosphere-thermosphere coupling.

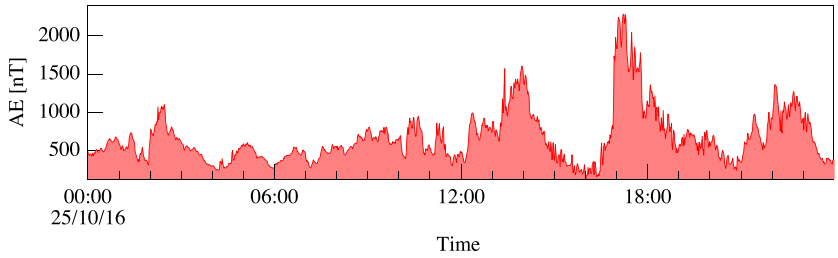

Figure 1. AE index values (1-min time resolution) during 25 October 25 2016.

It has been argued that small-scale FACs are probably randomly oriented due to their possible filamentary structure, while the FACs on the large-scale tend to be organized in sheets. These sheets tend to break up into individual filaments due to the development of multiscale magnetic structures in the form of flux tubes and consequently to the development of turbulence. These structures are somewhat similar to those found, for example, in a fluid flow with adjacent layers of different velocities when the Kelvin-Helmholtz instability develops (see, e.g., Keller et al., 1999, and references)

The aim of this work is to analyze the turbulent and intermittent nature of small-scale spatiotemporal magnetic field fluctuations in the high-latitude ionospheric regions where FACs flow, as a function of the geomagnetic activity disturbance level, and to discuss the relevance of the observed features with respect to an inhomogeneous structure of these currents. In the Earth's ionosphere, the turbulence may, indeed, be able to generate/create magnetic and plasma structures that can strongly affect plasma homogeneity, thus playing a relevant role in the FACs topology.

2. Data and Processing Approach

This study is based on in situ magnetic field observations from one of the three Swarm satellites, Swarm A.

The Swarm constellation consists of three identical satellites, which fly in two different orbital planes at two different altitudes. Two satellites (Swarm A and Swarm C) fly side by side at a mean altitude of approximately 460 km in a plane of 87.4° inclination during the considered time interval. The third satellite (Swarm B) orbits at a higher altitude than the others, flying about 50 km above in a plane of 88° inclination (Friis-Christensen et al., 2006). Each satellite is equipped with identical instruments: an absolute scalar magnetometer (ASM), a vector field magnetometer (VFM), an accelerometer (ACC), and an electric field instrument (EFI) comprising two thermal ion imagers (TIIs) and two Langmuir probes (LPs) (Knudsen et al., 2017).

Being interested in the analysis of the properties of the low-frequency magnetic field fluctuations in the regions of FACs, we select a day characterized by a mid-high geomagnetic activity level according to the auroral electroject (AE) index. The selected day is 25 October 2016, during which the AE index ranges from 125 to $\sim$ 2300 nT ($\langle \mathrm{AE} \rangle \sim 660$ nT) (see Figure 1). This day is characterized by quite variable interplanetary conditions with a B_Z^{GSM} mainly negative ($\langle B_Z^{GSM} \rangle = -2.2$ nT), a solar wind speed that increases from $\sim$ 400 km (slow solar wind) in the first half of the day, to $\sim$ 700 km (fast solar wind) in the second half of the day. Differently, low latitudes are characterized by a low geomagnetic activity ($SYM - H \in [-81, -21]$ nT).

For this day, we consider the Level 1b high-resolution (50 Hz) magnetic field data along the three magnetic components (X, Y, and Z in the North-East-Center frame of reference) sampled by the fluxgate magnetometer onboard of Swarm A. We use the *SW_OPER_MAGA_HR_1B* file type according to European Space Agency (ESA) nomenclature, which is available at ftp://swarm-diss.eo.esa.int.

To be able to investigate, separately, the properties of the magnetic fields generated in the northern polar region by the horizontal and FACs, we evaluate the components parallel and perpendicular to the direction of the main magnetic field of external, that is, magnetospheric and ionospheric, origin. Indeed, the FACs (Birkeland currents) are expected to produce a magnetic field perturbation which is perpendicular to the main geomagnetic field while the currents flowing horizontally in the *E* layer of the ionosphere (AEs) generate a magnetic field perturbation observed along the geomagnetic field lines (i.e., they produce vertical perturbations) near the current edges (Olsen, 1996). It follows the need to rotate measurements to a new

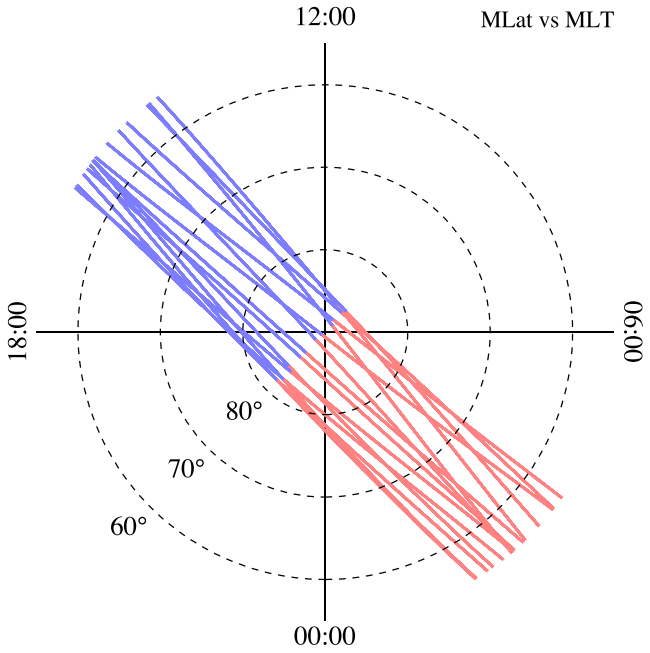

Figure 2. Polar crossings of the Swarm A satellite in the Northern Hemisphere during 25 October 2016. The polar view map is in magnetic local time (MLT) and quasi-dipole magnetic latitude (MLat) in the range from 55°N to 90°N. The colors identify the crossings in the dayside (blue) and nightside (red), respectively. Dashed circles are drawn at magnetic latitudes of 60°, 70°, and 80°.

frame with axes parallel and perpendicular to the main field. In detail, the parallel component ($b_{||}$) is locally nearly coincident with the Z component, while the two perpendicular ones are almost along the X ($b_{\perp,1}$) and Y ($b_{\perp,2}$) components.

Operationally, we remove the contributions coming from the core and crust, as modeled by CHAOS-6 (Finlay, 2015), from the Earth's magnetic field observed onboard Swarm A. In this way, we are able to exploit the contribution to the geomagnetic field due to sources located in the ionosphere and magnetosphere only. The obtained residuals in the North-East-Center frame of reference are successively rotated into the new frame and the components parallel and perpendicular to the direction of the main field evaluated.

Figure 2 shows a polar view map in magnetic local time (MLT) and quasi-dipole magnetic latitude of the polar crossings of Swarm A satellite in the Northern Hemisphere during the selected day (25 October 25 2016). The two colors identify the crossings in the dayside (blue) and nightside (red), respectively.

Figure 3 displays, in the top panel, an example of the magnetic field of external origin along the components perpendicular and parallel to the main field, estimated for one crossing over the Northern Hemisphere. In the bottom panel of the same figure, the FAC density is reported for the same interval. The reported FAC density is a Swarm Level-2 (L2-FAC) single-spacecraft product (Ritter et al., 2013) obtained by considering the Swarm A satellite. It is calculated from the spatial gradients of the magnetic field observed along the direction defined by the spacecraft orbit track (Ritter et al., 2013), and it is automatically estimated and available at ftp://swarm-diss.eo.esa.int (*FACATMS_2F* file type). The knowledge of the position of the FACs during the crossings of the northern high-latitude regions by Swarm A satellite allows the extraction from the broad dataset of the parallel and perpendicular magnetic field perturbations for 25 October, which are associated with FAC regions.

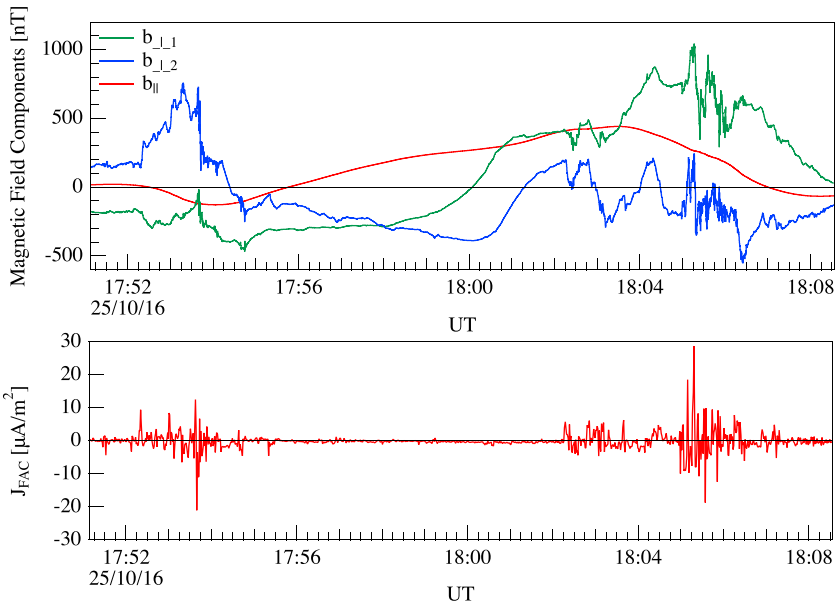

Figure 3. Top panel: an example of the magnetic field of external origin along the perpendicular and parallel components to the main field along a single crossing of the northern polar region. Bottom panel: the density of the field-aligned currents obtained as product of Level-2 (L2-FAC) from the data collected by the Swarm A satellite.

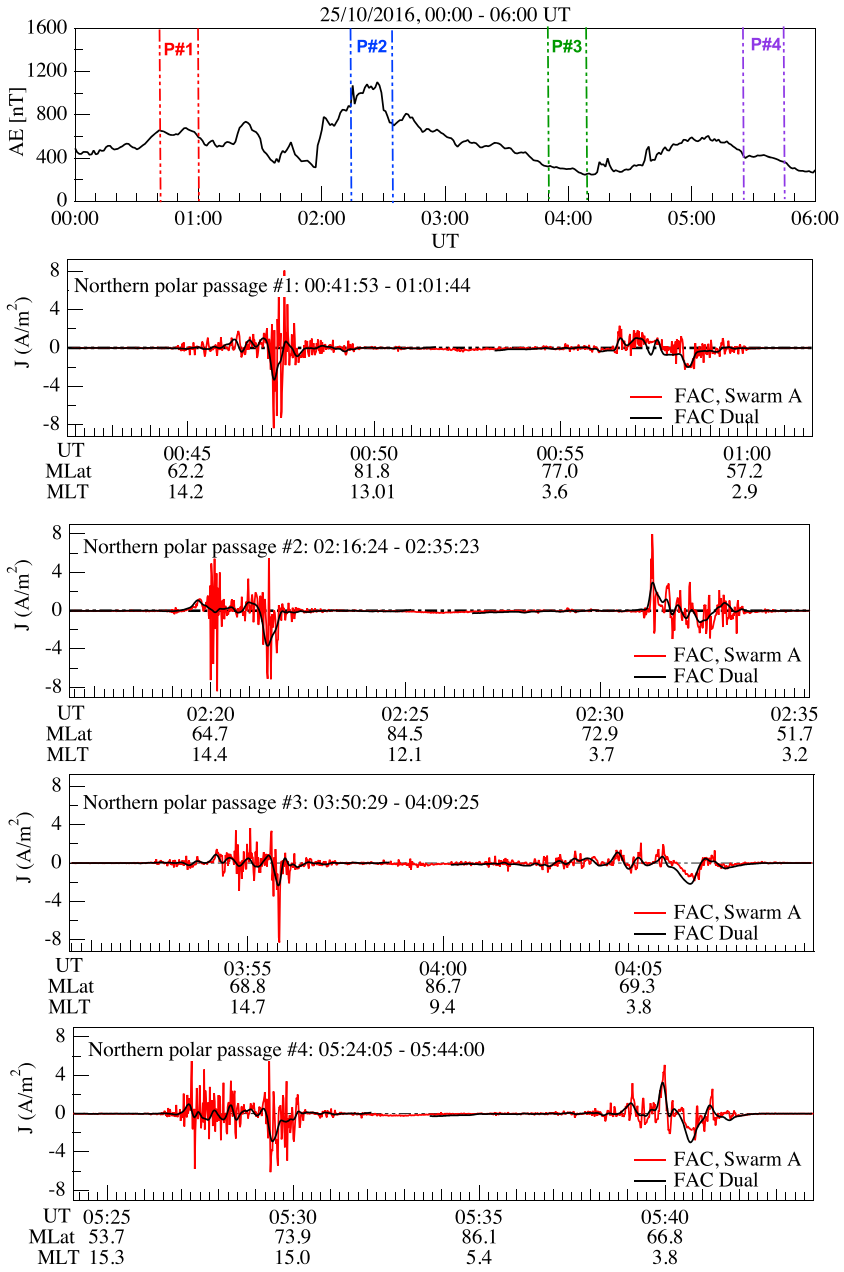

Figure 4. Comparison between the two Level-2 FAC data (single- and dual-satellite FACs) for the first four of the 15 crossings of the northern high-latitude regions occurring on 25 October 2016. The top panel shows the first four selected crossings (P#1, P#2, P#3, and P#4 reported in the four successive panels) and the corresponding values of the AE index.

Recently, Lühr et al. (2016) showed that some FAC structures can be missed using the single-spacecraft magnetic field measurements and that the dual-satellite approach is capable of detecting some of these missed structures, thus improving the FAC observations. However, according to Lühr et al. (2016), most of the events missed by the single-spacecraft technique appear on the nightside and poleward of the auroral oval. Thus, to check that the selected intervals correctly identify the FAC regions, we also consider the dual-spacecraft FACs estimate from the pair Swarm A/C during all the crossings of the high-latitude regions.

Figure 4 displays the comparison between the two Level-2 FAC data (single- and dual-satellite FACs) for the first four of the 15 crossings of the northern high-latitude regions occuring on 25 October 2016. No

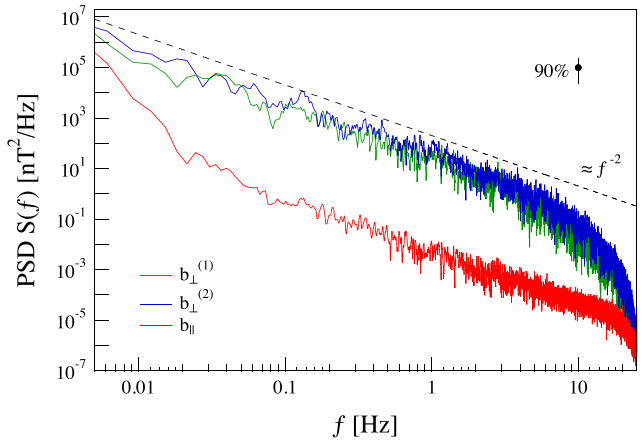

Figure 5. The PSDs of the magnetic field fluctuations along the three directions: two perpendicular and one parallel to the main field. PSDs are reported as a function of frequency and display a power law decay over about three decades. The dashed line is a power law dependence with exponent $\alpha = 2$. The error bar in the annotation refers to the 90% confidence interval in estimation of PSD.

discrepancies are observed between the position of FACs obtained by the two different techniques. Although FACs are characterized by different amplitudes, both products locate FACs in the same spatial regions.

In practice, to limit our analysis to the regions where the FACs flow, we select only those time intervals where the local (time window of 10 s) standard deviation σ_{std} of the single-spacecraft current (product L2-FAC for Swarm A) is > 0.03 A/m^2. The value of $\sigma_{std} \sim 0.03$ A/m^2 is the optimal value obtained by a statistical analysis over the entire considered data set, which better identifies the border of the FAC regions. The analysis of the nature of the fluctuations of the magnetic field residuals will be made only for these time intervals.

3. Analysis and Results

To study the nature of the small-scale low-frequency magnetic field fluctuations, we perform the analysis of the selected data set in the temporal domain and evaluate the spectral and scaling features of these small-scale magnetic field fluctuations. This means that we investigate the power spectral densities (PSDs), the structure functions ($S_q(\tau)$), and the relative scaling of the scaling exponents ($\xi(q)$) as a function of the moment order (q) for the external magnetic field components, perpendicular and parallel to the main field (as it will be demonstrated in more detail in the next section, the spacecraft observed that low-frequency temporal magnetic field fluctuations are dominated primarily by the Doppler-shifted and essentially stationary spatial variations of the field-aligned filamentary current structures. Thus, the time scale τ and frequency f discussed in this section may be viewed essentially as spatial scale $\delta \sim v_{sp}\tau$ and mode number $k \sim 2\pi f/v_{sp}$ with v_{sp} being the spacecraft velocity).

To begin, we investigate the average PSDs of the fluctuations of the magnetic field residuals. The PSD would provide us information on the existence of a possible inertial/scaling range, which should manifest in a power law behavior of PSD over a wide range of scales (Biskamp, 2003; Frisch, 1995; Kolmogorov, 1941a; 1941b).

Figure 5 displays the PSDs of the magnetic field along the perpendicular and parallel components as a function of frequency (f). The PSDs have been obtained using all our data set regardless of the position of the satellite with respect to the Sun (dayside/nightside). These PSDs can be consequently considered as time averages on the selected polar hemisphere crossings. The spectral features are characterized by power laws ($S(f) \propto f^{-\alpha}$) that span more than three decades of frequency (0.005 Hz$< f < 4 \div 8$ Hz) with spectral exponents α that lie in the range $\alpha \simeq 2.0 \sim 2.5$. A clear difference in the energy content between parallel and perpendicular fluctuations is observed, while no relevant differences in the PSDs are observed between the two perpendicular directions inside the 90% confidence interval. Similar values have been found by Golovchanskaya et al. (2006) analyzing magnetic field observations by the DE2 satellite crossing the FAC regions in the polar ionosphere. Furthermore, as already discussed in Rother et al. (2007), the break near $4 \div 8$ Hz in the PSDs could be attributed to the fine structure of the FACs.

Figure 6 shows the same analysis, but this time separated into dayside and nightside crossings of FACs in the case of the two perpendicular components. A clear difference in the spectral law behavior is observed between dayside and nightside fluctuations; the dayside spectrum is less steep than the nightside one suggesting a less persistent nature of fluctuations.

Figures 5 and 6 show that the spectral exponents are larger than 2 in the analyzed range of frequencies. Similar results have been found by Chaston et al. (2008) analyzing the magnetic and electric field fluctuations in the auroral oval using measurements onboard of the FAST satellite.

It is worth nothing that the observed spectral exponents are larger than what is generally expected for 3D magnetohydrodynamic (MHD) turbulence. Indeed, for ideal MHD turbulence, the spectral exponent is expected in the range $\alpha \in (3/2, 5/3)$ as predicted by Iroshikov-Kraichnan and/or Kolmogorov theory of MHD and/or fluid turbulence (Biskamp, 2003; Bruno & Carbone, 2016; Frisch, 1995). This discrepancy could be due to a strong anisotropy of the fluctuations as also suggested by the different energy content of

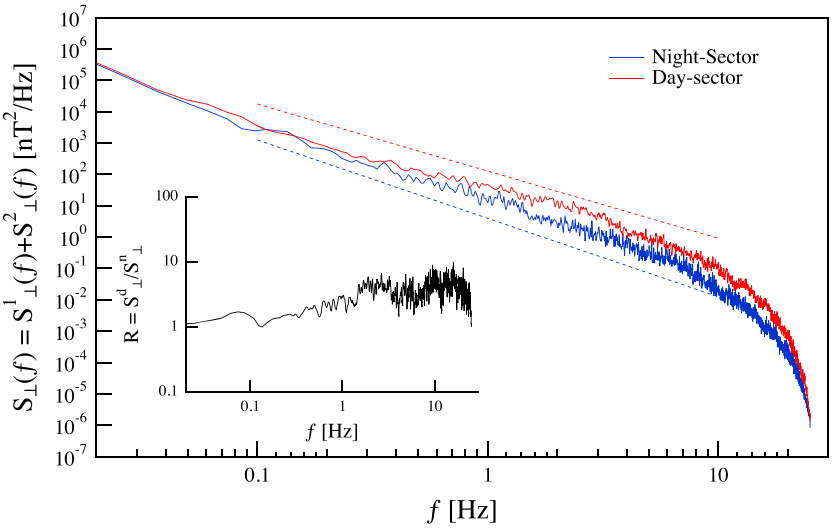

Figure 6. The average PSDs of the magnetic field fluctuations along the perpendicular components for the dayside and nightside crossings of FAC regions. PSDs show a slight different behavior with the frequency in terms of the observed spectral exponents ($\alpha \sim 2.1 \div 2.2$ in the dayside sector and $\alpha \sim 2.5 \div 2.6$ in the nightside sector—see dashed lines). The inset shows the ratio between the dayside and the nightside PSDs.

fluctuations of the magnetic field residual in the parallel and perpendicular directions to the main field. Indeed, as shown in Figure 5, the fluctuations in the parallel direction are strongly reduced in comparison with perpendicular ones. This can be easily realized by analyzing the ratio, $R(f)$, between the perpendicular and parallel PSDs as a function of frequency (see Figure 7). The ratio $R(f)$, which is defined according to the following expression

$$R(f) = \frac{S^1_\perp(f) + S^2_\perp(f)}{2S_{||}(f)}, \tag{1}$$

clearly shows that the energy spectra associated with the perpendicular components of the magnetic field fluctuations are characterized by values greater than those relative to the energy spectrum associated with the parallel component. This result suggests that turbulent fluctuations are restricted to a plane that is perpendicular to the main geomagnetic field local direction, thus indicating a possible reduction of the dimensionality of the turbulence, which in first approximation can be supposed to be quasi-bidimensional (2D). This means that the turbulent cascade occurs preferentially in the direction perpendicular to the main field. This view is also in agreement with the lack of plasma particle collisions at the Swarm altitudes that implies the conductivity tensor off-diagonal elements to be essentially negligible, forcing the current to flow parallel to the main geomagnetic field direction.

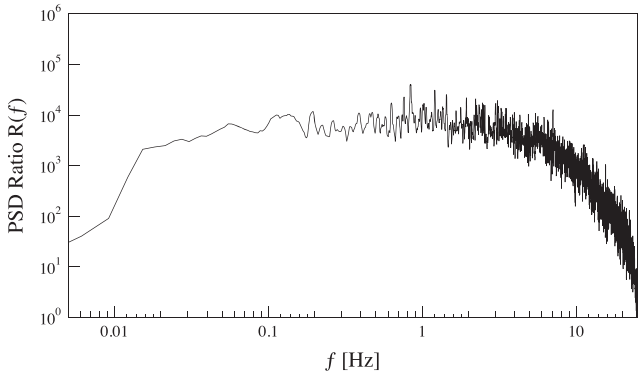

Figure 7. Ratio, $R(f)$, between the normalized and time-averaged perpendicular and parallel energy spectra as a function of frequency.

The hypothesis of a 2D turbulence is also supported by the low values of the plasma β (the ratio of the plasma pressure to the magnetic pressure), $\beta \sim 10^{-3} - 10^{-4}$, which characterize these regions. In this configuration, the magnetic fluctuations are, indeed, essentially confined to a plane perpendicular to the mean field, since field lines resist to bending in the parallel direction (Biskamp, 2003).

A possible explanation of the steeper PSDs observed in the case of magnetic field fluctuations in the FACs regions can be traced by simple dimensional arguments. In 3D fluid turbulence, K41 Kolmogorov's theory predicts a -5/3 spectral dependence for homogeneous and isotropic turbulence. On the other hand, the Iroshnikov-Kraichnan theory for Alfvénic 3D turbulence predicts a power spectral density with a spectral exponent $\alpha = -3/2$. In these two cases, the dimensionality of the turbulence in terms of number of free variables (degrees of freedom) is expected to be 3 and 4 for fluid and MHD turbulence, respectively. Now, the scaling properties of turbulent media are generally described in terms of qth-order structure functions, S_q, that is, the moments of the signal increments at different spatial scales, and their scaling with the different spatial scales. In particular, the corresponding qth-order structure functions are expected to scale as $q/3$ and $q/4$ for homogeneous fluid and MHD turbulence, respectively, that is,

$$S_q(\delta r) = \langle |x(r + \delta r) - x(r)|^q \rangle \sim \delta r^{\gamma(q)}, \tag{2}$$

where x is the variable under investigation, δr is a spatial shift, and $\gamma(q) = q/3$ or $q/4$. In such a framework, the spectral exponent α is expected to be related to the second-order structure exponent by the following relation (via the Wiener-Khinchine theorem),

$$\alpha = 1 + \gamma(2), \tag{3}$$

so that we get $\alpha = 5/3$ and $3/2$ for fluid and MHD turbulence, respectively. Taking into account that the fluctuations are essentially 2D in the FAC regions, if we suppose that these fluctuations are of Alfvénic nature (so that due to the Alfvénic correlation between $\vec{v}$ and $\vec{b}$ fluctuations the degree of freedom reduces to 2), since they can be described in terms of Taylor force-free MHD equilibrium, we can expect that for 2D homogeneous fluctuations, the qth-order scaling exponent is $q/2$. Consequently, $\gamma(2) = 1$ and the spectral exponent is expected to be $\alpha = 2$. This result is not far from what is observed in terms of average properties (see Figure 5). Clearly, intermittency corrections and/or anisotropic features in the plane perpendicular to the main magnetic field could modify the expected spectral exponent. In particular, the presence of anisotropy in the plane perpendicular to the main magnetic field could reduce the dimensionality of the fluctuation field, so that the effective dimension could be $D < 2$.

Moving to the analysis of the scaling features of magnetic field fluctuations, we concentrate our attention to the perpendicular components, which are expected to be strongly correlated with the structure of the FACs. Thus, we compute the so-called generalized structure functions of the magnetic field perpendicular components as a function of delay time τ, that is,

$$S_q(\tau) = \langle |b_i(t + \tau) - b_i(t)|^q \rangle, \tag{4}$$

where b_i is the i^{th}-component of the magnetic field residual, τ is the delay time, and $\langle \dots \rangle$ stands for a statistical average. For a scaling process, a power law behavior is expected, that is,

$$S_q(\tau) = \tau^{\xi(q)}, \tag{5}$$

where $\xi(q)$ are the scaling exponents of the structure functions. In the case of simple fractal signals/structure, these exponents are expected to be a linear function of the moment order q. Conversely, for more complex fractal signals/structures, such as inhomogeneous multifractals, the scaling exponents $\xi(q)$ show a departure from a linear dependence on the moment order q, being generally a convex function of q. This type of analysis can be applied in our study because, although the time series are nonstationary, they are characterized by stationary increments (Davis et al., 1994; Mandelbrot et al., 1997). The PSDs of the time series relative to the increments of the magnetic field fluctuations along the parallel and perpendicular components, shown in Figure 8, are indeed characterized by quasi-flat spectral densities at frequencies below 5–10 Hz, which support the stationary character of the field increments (Davis et al., 1994).

Figure 9 shows the average qth-order structure functions, $S_q(\tau)$, for different moments q as a function of the time delay τ relatively to dayside/nightside crossings of FAC regions. In this case, we use all available data

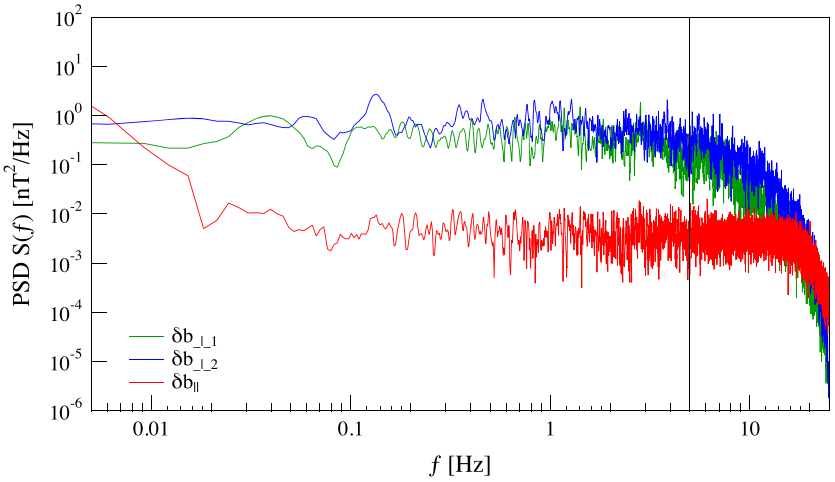

Figure 8. Power spectral density (PSD) of the increments of the magnetic field fluctuations along the three components: two perpendicular and one parallel to the main field. PSDs are expressed as a function of frequency and display a quasi-flat spectrum at frequencies less than 5 Hz.

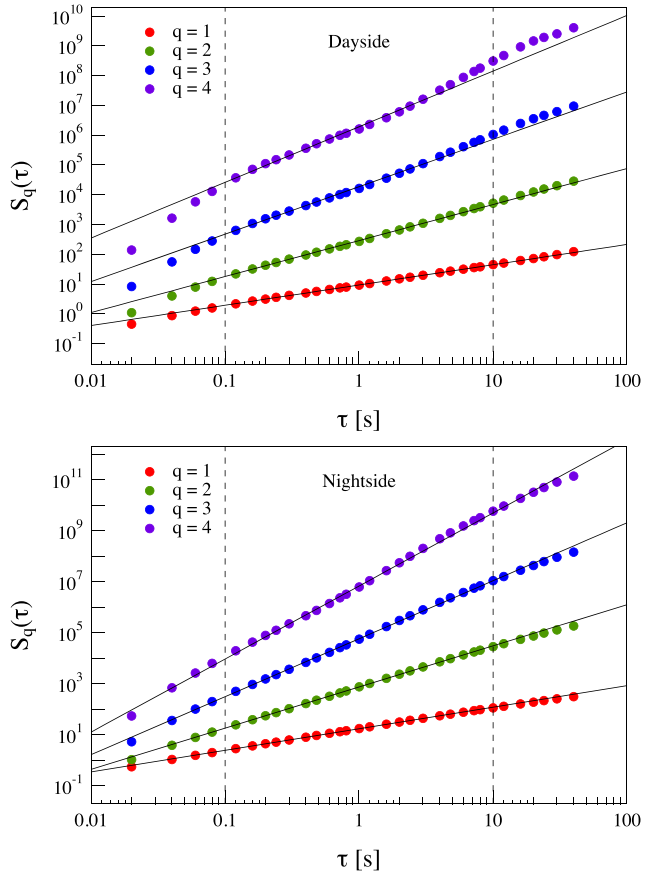

Figure 9. Average structure functions, $S_q(\tau)$, derived from the increments of the external magnetic field in the directions perpendicular to the main field, for moment q from 1 to 4 for dayside (upper panel) and nightside (lower panel) crossings. The two dashed lines delimit the region where the power law behavior is considered for estimating the scaling exponents.

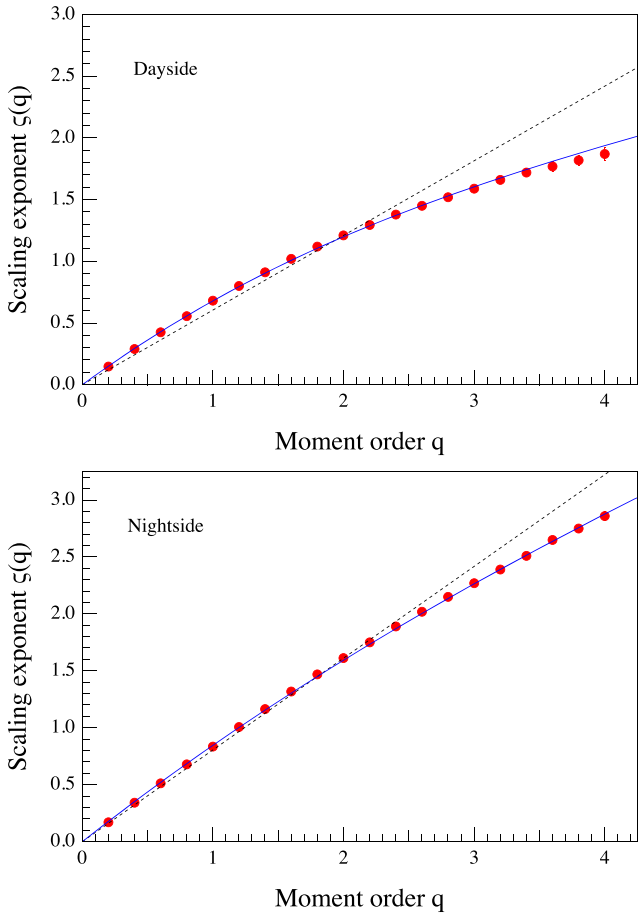

Figure 10. Behavior of the scaling exponents $\xi(q)$ relative to the structure functions of the increments of the magnetic field residuals in the plane perpendicular to the main field recorded during the dayside (upper panel) and nightside (lower panel) crossings of FACs. The dashed lines refer to linear scaling (monofractal behavior) while blue curves are related to the generalized P-model.

relative to the magnetic field fluctuations along the perpendicular directions to the main field. To compute the average structure functions, the increments of each crossing are normalized by the standard deviation of the increments at the smallest timescale ($\tau = 0.02$ s). This operation is done in order to weight correctly the structure functions of the different FAC crossings when evaluating the average scaling features. Power law behavior of $S_q(\tau)$ is observed for all qs in the range $\sim 0.1 < \tau < 10$ s. The lower limit is related to the maximum frequency, $f_{max} \sim 1/2\tau \sim 5$Hz, where a flat spectrum is observed. We stress that the range of scales, here investigated, is out of the PSD high-frequency spectral break, possibly related to intense kilometer-scale FACs (Rother et al., 2007).

The values of the scaling exponents $\xi(q)$ of the qth-order structure functions, $S_q(\tau)$, estimated by using a least-square fitting in the range $\sim 0.1 < \tau < 10$ s are reported in Figure 10 for moment $q \in [0, 4]$. Here, two different panels are presented. In the upper panel, we show the scaling exponents, $\xi(q)$, relative to the dayside crossings of FACs, while in the lower panel, the same quantities for nightside crossings of FACs are shown.

For both dayside and nightside crossings of FAC regions, the magnetic field increments show anomalous scaling properties. Indeed, the values of the scaling exponents $\xi(q)$ are not characterized by a linear dependence on q, and that marks the occurrence of anomalous scaling features, that is, a multifractal structure of the magnetic field fluctuations. This is the evidence for the occurrence of intermittency. Intermittency is a very peculiar feature of fluid and magnetohydrodynamic turbulence (Biskamp, 2003; Bruno & Carbone, 2016; Frisch, 1995). This property is the consequence of the local nature of the ideal Richardson's cascade due to its stochastic nature (Landau's remark on the Kolmogorov/Obukhov K41 theory of turbulence

(Kolmogorov, 1962; Frisch, 1995)) so that the resulting dissipation field is no longer homogeneous in terms of scaling its features (Frisch, 1995). In other words, intermittency is a manifestation of a multifractal structure of the dissipation field, that is, the dissipation is sporadically localized in the space (and also in time).

To better characterize the deviation from linearity of the observed scaling exponents $\xi(q)$, we compare it with the expected behavior predicted by a generalized two-scale Cantor set or P model. In the case of 3D fully developed fluid and MHD turbulence, the anomalous scaling of the exponent of the qth-order structure function as a function of the moment order q can be modeled by the P model (Meneveau & Sreenivasan, 1987), which predicts

$$\xi(q) = 1 - \log_2\left(p^{\frac{q}{3}} + (1-p)^{\frac{q}{3}}\right) \tag{6}$$

and

$$\xi(q) = 1 - \log_2\left(p^{\frac{q}{4}} + (1-p)^{\frac{q}{4}}\right) \tag{7}$$

for the fluid and MHD turbulence, respectively. In our case, the dimensionality of the observed turbulent fluctuations is neither 3 nor 4, so we can try to fit the observed behavior of $\xi(q)$ by a generalization of the last two expressions, that is,

$$\xi(q) = 1 - \log_2\left(p^{\frac{q}{d}} + (1-p)^{\frac{q}{d}}\right), \tag{8}$$

where the parameter d is representative of an effective dimension of the fluctuation field. Figure 10 reports the fit of the trend $\xi(q)$ using the generalized P model (see Equation (8)). The fits are excellent for both dayside and nightside sectors. The fitting parameters are $p = [0.76 \pm 0.01]$ and $d = [1.58 \pm 0.01]$ for dayside FAC crossings and $p = [0.66 \pm 0.01]$ and $d = [1.20 \pm 0.01]$ for nightside FAC crossings, respectively. In both cases, the parameter $p \neq 0.5$, indicating that the fluctuation field is not homogeneous (i.e., we are in the presence of an inhomogeneous dissipation pattern). The higher value of the p parameter for the dayside FAC sector supports the higher degree of intermittency of fluctuations/increments in that region. Furthermore, the observed effective dimension, d, is higher in the dayside than in the nightside, suggesting a different degree of correlation of the fluctuations in the perpendicular direction to the main magnetic field. We note that the effective dimensions agree very well with the observed spectral exponents as $\alpha = 2/d + 1$ ($\alpha \sim 2.2$ and ~ 2.6 for dayside and nightside sectors, respectively).

Thus, the magnetic field fluctuations in the FAC regions are characterized by an intermittent turbulence that tends to localize large fluctuations (i.e., energy) in small spatial regions, or "hot spots." Furthermore, the obtained results provide the evidence that this intermittent character (anomalous scaling) is higher in the dayside sector than in the nightside one.

4. Discussion and Conclusions

We have investigated the nature of the magnetic field fluctuations in the topside F region of the ionosphere using the high-resolution (50 Hz) magnetic field measurements recorded by the Swarm ESA's Earth observation mission. In detail, we have carefully examined the small-scale low-frequency magnetic field fluctuations in the high-latitude ionospheric regions, associated with the FACs. For this reason, we have analyzed the components of the magnetic field residual of external origin with directions parallel and perpendicular to the main field and evaluated the spectral and scaling features of these small-scale magnetic field fluctuations recorded in the FAC regions.

From our study, the following conclusions emerge:

- as expected the magnetic field fluctuations/increments are strongly anisotropic (see Figure 5) and essentially confined to the plane perpendicular to the main field, suggesting that the fluctuations are essentially 2D;
- the spatiotemporal magnetic field fluctuations in the perpendicular plane show scale invariance over nearly two and half orders of magnitude (see Figure 9), which is one of the properties of observed turbulence;
- the obtained scale invariance is anomalous (see Figure 10), suggesting the occurrence of intermittency, that is, large amplitude fluctuations that are strongly localized in the space and time; and

- the intermittent character (anomalous scaling) exhibits a dependence on MLT sectors displaying a significant increase in the dayside (see Figure 10).

These results support the idea of the occurrence of intermittent turbulence in the regions of FACs. The observed spectral character of a 2D turbulence resembles the numerical results of 2D ideal compressible MHD simulations by Chang et al. (2004), which found the formation of a spectral domain $S(k) \sim k^{-2}$. Clearly, the similarity between our results and Chang et al. (2004) 2D MHD simulations requires the assumption that Taylor's hypothesis is valid, that is, that the frequency f, measured in the spacecraft reference system, is related to the wave number k by the simple relationship $2\pi f \sim v_{sp}k$, where v_{sp} is the spacecraft speed ($\sim$ 8 km/s). This hypothesis has been shown to be reasonable for the crossing of FAC regions and in other works dealing with observations of turbulence in auroral regions (see e.g., Chaston et al., 2008 and references therein). Actually, to be more precise, this hypothesis is different from the Taylor hypothesis argument in the solar wind, where the solar wind moves much faster than that of the spacecraft. Indeed, according to 2D MHD calculations of the inertial Alfvenic fluid equations, the interacting coherent structures form nearly 2D static potential structures, and thus, as a satellite moves across these nearly static structures, they exhibit low-frequency fluctuations due to Doppler shifts. Furthermore, the range of investigated timescales (from 0.1 up to 10 s) deals with time intervals where it can be reasonably assumed that the structures are mainly frozen, as also reported in other papers (e.g.,De Michelis et al., 2017; Gjerloev et al., 2011). Indeed, it has been clearly shown that in the dayside/nightside sectors, the FAC structures are nearly stable up to 60/160 s, respectively. In other words, we assume that the structures do not evolve in time during the spacecraft crossing at the investigated range of scales. This assumption is supported by the previous discussion on the link between the Doppler shift and fluctuation in the low-frequency range reported in section 3 (see also Kintner & Seyler, 1985). Furthermore, we can expect that the evolution time for structures in a turbulent medium could be longer than that of the typical nonlinear time associated with the corresponding wavenumber. This is also confirmed by looking at the PSD of field increments (see Figure 8), which displays a quasi-flat behavior in the range of the investigated timescales, supporting a quasi-stationarity condition.

Due to the strong magnetic field in the polar regions and to its quasi-uniform and unidirectional character, the variations/perturbations along the main geomagnetic field direction are damped by the plasma dynamics in the parallel direction (Biskamp, 2003). In this picture, the field is essentially potential and a reasonable approximation to describe the emerging scenario is the *Reduced Magneto-Hydro-Dynamics* (RMHD) (refer to Biskamp, 2003). The magnetic field fluctuations, although small, dominate in the perpendicular directions with respect to the mean magnetic field B_0, and thus, they can be described by a flux function, $\psi(x, y)$, that is,

$$\mathbf{B} = \mathbf{e}_z \times \nabla\psi + B_0\mathbf{e}_z \quad \rightarrow \quad \mathbf{B} = (\delta B_x, \delta B_y, B_0), \tag{9}$$

where the z direction is aligned to the mean field and $B_0 \equiv B_z$ is assumed to be constant and large with respect to the perpendicular field, $B_\perp/B_z \ll 1$. Here the flux function ψ, which is associated with the poloidal field, is essentially the axial component of the vector potential A_z, that is, $\psi = -A_z$, and represents the magnetic field flux. The nearly force-free condition for the mean field and the current density conservation, $\nabla \cdot \mathbf{J} \sim 0$, imply that $\mathbf{B} \cdot \nabla J_z \sim 0$ (see Chang et al., 2004), that is,

$$B_0 \frac{\partial J_z}{\partial z} = -\left(\frac{\partial \psi}{\partial y}\frac{\partial}{\partial x} - \frac{\partial \psi}{\partial x}\frac{\partial}{\partial y}\right) J_z + \ldots, \tag{10}$$

where the ellipsis indicates the possible occurrence of other nonideal terms which are associated with some modifying effects. Neglecting the ellipsis and including Ampere's law, a simple solution of Equation (10) for the axial current J_z and the flux function ψ is the class of circularly cylindrical field-aligned flux tubes (see Figure 11), which can be considered as coherent structures (Chang et al., 2004; Wu & Chang, 2000, 2001). The dynamics of these coherent structures can strongly affect the local plasma and magnetic field topologies and can be a possible source of the observed intermittent turbulent fluctuations. On the other hand, the formation of multiscale coherent field-aligned structures implies the generation of a very complex pattern of the current density J_z, which may result to be strongly inhomogeneous in the direction perpendicular to the mean magnetic field. We note how this scenario is compatible with approximate force-free equilibrium, $\nabla \times \mathbf{B} \sim \theta\mathbf{B}$ (here θ is a constant), which is a minimal free-energy condition according to the Woltjer theorem. In this framework, the potential structures should explain the observed nearly field-aligned interacting current filaments that in turn produce the corresponding low-frequency magnetic fluctuations.

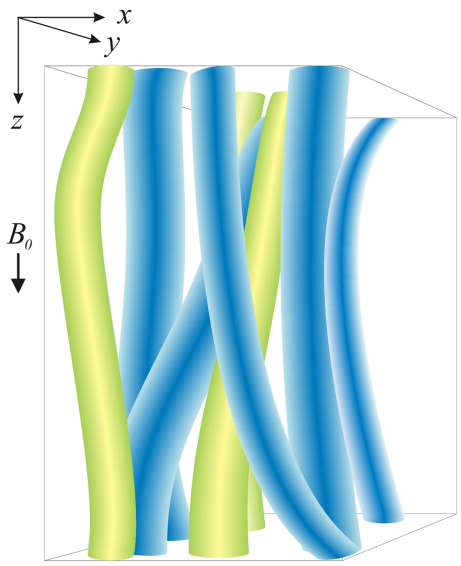

Figure 11. A sketch of coherent field-aligned flux tubes in a quasi force-free equilibrium. The current is aligned along magnetic structures. The colors refer to different directions of the field-aligned currents.

Thus, low-frequency satellite magnetic field measurements provide nearly 2D spatial fluctuating signatures (see e.g., Tam Sunny et al., 2010). However, due to the sporadic interactions among the filamentary structures generated by the nonideal dissipative effects and the complexity phenomenon of coarse-grained dissipation (Chang et al., 2004), entrained within these nearly stationary spatial structures, there are probably small fractions of temporal fluctuations, some random/stochastic and some with electrostatic/electromagnetic ion cyclotron or inertial/kinetic Alfvén wave characteristics.

This scenario can pave the way to a better understanding of the nature of the small-scale FACs observed throughout the auroral oval (Lühr et al., 1994; Neubert & Christiansen, 2003; Stasiewicz & Potemra, 1998) which, as suggested by the presence of 2D intermittent turbulence of the magnetic field fluctuations associated with these currents, could be filamentary and inhomogeneous. Thus, our results seem to support the previous hypothesis according to which the FACs on small scales are randomly oriented, thus reflecting a filamentary structure (Neubert & Christiansen, 2003).

However, all this picture is strongly dynamic, so that the current field pattern and the associated magnetic field structures are continuously evolving. This is the origin of the observed intermittent turbulence.

Really, we cannot exclude that there are also other possible scenarios compatible with what found, such as the occurrence of electrostatic turbulent fluctuations in dynamical equilibrium with **E×B** drift velocity shear (as it occurs in tokamak edge turbulence), which exhibits strong intermittency and formation of coherent structures, playing a relevant role in driving energy losses (see e.g., Golovchanskaya et al., 2006; Lepreti et al., 2009; Tam Sunny et al., 2005, and references therein).

The validation of the most appropriate scenario requires the investigation of other physical quantities and multifractal properties such as those described in the monograph by Chang (2015) and will be the topic of a future work.

Acknowledgments
The results presented rely on data collected by one of the three satellites of the Swarm constellation. We thank the European Space Agency (ESA) that supports the Swarm mission. Swarm data can be accessed online at http://earth.esa.int/swarm. The authors kindly acknowledge V. Papitashvili and J. King at the National Space Science Data Center of the Goddard Space Flight Center for the use permission of 1 min OMNI data and the NASA CDAWeb team for making these data available at https://cdaweb.gsfc.nasa.gov/index.html/. This work is supported by ESA under contract ESA Contract No. 4000125663/18/I-NB (INTENS).

References

Anderson, B. J., Korth, H., Waters, C. L., Green, D. L., & Stauning, P. (2008). Statistical Birkeland current distributions from magnetic field observations by the Iridium constellation. *Annals of Geophysics*, *26*, 671–687. https://doi.org/10.5194/angeo-26-671-2008

Anderson, B. J., Ohtani, S.-I., Korth, H., & Ukhorskiy, A. (2005). Storm time dawn-dusk asymmetry of the large-scale Birkeland currents. *Journal of Geophysical Research*, *110*, A12220. https://doi.org/10.1029/2005JA011246

Angelopoulos, V., Mukai, T., & Kokubun, S. (1999). Evidence for intermittency in Earth's plasma sheet and implications for self-organized criticality. *Physics of Plasmas*, *6*, 4161.

Birkeland, K. (1908). *The Norwegian Aurora Polaris Expedition, 1902-1903.* (Vol. 1). H, Aschehoug & Co., Christiania.

Biskamp, D. (2003). *Magnetohydrodynamic turbulence*. New York NY: Cambridge University Press.

Booker, H. G. (1956). Turbulence in the ionosphere with applications to meteor-trails, radio-star scintillation, auroral radar echoes, and other phenomena. *Journal of Geophysical Research*, *61*(4), 673.

Borovsky, J. E., Elphic, R. C., Funsten, H. O., & Thomsen, M. F. (1997). The Earth's plasma sheet as a laboratory for flow turbulence in high-β MHD. *Journal of Plasma Physics*, *57*, 1–34.

Bruno, R., & Carbone, V. (2016). Turbulence in the solar wind, *Lect. Notes Phys.* (pp. 928). Switzerland: Springer. https://doi.org/10.1007/978-3-319-43440-7

Chang, T. (2015). *An introduction to space plasma complexity*. New York NY: Cambridge University Press.

Chang, T., Tam, S., & Wu, C.-C. (2004). Complexity induced anisotropic bimodal intermittent turbulence in space plasmas. *Physics of Plasmas*, *11*, 1287–1299.

Chang, T., Tam, S., Wu, C.-C., & Consolini, G. (2003). Complexity, Forced and/or Self-Organized Criticality, and topological phase transitions in space plasmas. *Space Science Reviews*, *107*, 425–445.

Chaston, C. C., et al. (2008). The turbulent alfvénic aurora. *Physical Review Letters*, *100*(175003).

Cheng, Z. W., Shi, J. K., Dunlop, M., & Liu, Z. X. (2013). Influences of the interplanetary magnetic field clock angle and cone angle on the field-aligned currents in the magnetotail. *Geophysical Research Letters*, *40*, 5355–5359. https://doi.org/10.1002/2013GL056737

Chisham, G., et al. (2007). A decade of the Super Dual Auroral Radar Network (superDARN): scientific achievements, new techniques and future directions. *Surveys Geophysics.*, *28*, 33–109. https://doi.org/10.1007/s10712-007-9017-8

Christiansen, F., Papitashvili, V. O., & Neubert, T. (2002). Seasonal variations of high latitude field-aligned currents systems inferred from Oersted and Magsat observations. *Journal of Geophysical Research*, *107*, 1029. https://doi.org/10.1029/2001JA900104

Cummings, W. D., & Dessler, A. J. (1967). Field-aligned currents in the magnetosphere. *Journal of Geophysical Research*, *72*, 1007–1013. https://doi.org/10.1029/JZ072i003p01007

Dagg, M. (1957). The origin of the ionospheric irregularities responsible for radio-star scintillations and spread-f-II: Turbulent motion in the dynamo region. *Journal of Atmospheric and Solar-Terrestrial Physics*, *11*, 139.

Davis, A., Marshak, A., Wiscombe, W., & Cahalan, R. (1994). Multifractal characterizations of nonstationarity and intermittency in geophysical fields: Observed, retrieved, or simulated. *Journal of Geophysical Research*, *99*, 8055–8072.

De Michelis, P., Consolini, G., & Tozzi, R. (2015). Magnetic field fluctuation features at Swarm's altitude: A fractal approach. *Geophysical Research Letters*, *42*, 3100–3105. https://doi.org/10.1002/2015GL063603

De Michelis, P., Consolini, G., Tozzi, R., Giannattasio, F., Quattrociocchi, V., & Coco, I. (2019). Features of magnetic field fluctuations in the ionosphere at Swarm altitude. *Annals of Geophysics*, *62*, GM499. https://doi.org/10.4401/ag.7789

De Michelis, P., Consolini, G., Tozzi, R., & Marcucci, M. F. (2017). Scaling features of high-latitude geomagnetic field fluctuations at Swarm altitude: Impact of IMF orientation. *Journal of Geophysical Research: Space Physics*, *122*, 10,548–10,562. https://doi.org/10.1002/2017JA024156

Finlay, C. C. (2015). DTU Candidate field models for IGRF-12 and the CHAOS-5 geomagnetic field model. *Earth Planets and Space*, *67*, 114.

Friis-Christensen, E., Lürh, H., & Hulot, G. (2006). Swarm: A constellation to study the earth's magnetic field. *Earth Planets Space*, *58*, 351.

Frisch, U. (1995). *Turbulence: The Legacy of A.N*. Kolmogorov: Cambridge University Press.

Gjerloev, J. W., Ohtani, S., Iijima, T., Anderson, B., Slavin, J., & Le, G. (2011). Characteristics of the terrestrial field-aligned current system. *Annals of Geophysics*, *29*, 1713–1729.

Golovchanskaya, I. V., Ostapenko, A. A., & Kozelov, B. V. (2006). Relationship between the high-latitude electric and magnetic turbulence and the Birkeland field-aligned currents. *Journal of Geophysical Research*, *111*, A12301. https://doi.org/10.1029/2006JA011835

Iijima, T. (1984). Field-aligned currents during northward IMF, *Geophysical Monograph Series: Magnetospheric currents* (pp. 28). Washington DC: American Geophysical Union. https://doi.org/10.1029/GM028p0115

Iijima, T., & Potemra, T. A. (1978). Large-scale characteristics of field-aligned currents associated with substorms. *Journal of Geophysical Research*, *83*(A2), 599–615. https://doi.org/10.1029/JA083iA02p00599

Iijima, T., Potemra, T. A., & Journal of Geophysical Research (1976). Field-aligned currents in the dayside cusp observed by Triad, *81*(34), 5971–5979. https://doi.org/10.1029/JA081i034p05971

Iijima, T., & Shibaji, T. (1987). Global characteristics of northward IMF-associated (NBZ) field-aligned currents. *Journal of Geophysical Research*, *92*, 2408.

Keller, K. A., Lysak, R. L., & Song, Y. (1999). A three-dimensional simulation of the Kelvin-Helmholtz instability. In S. Ohtani, R. Fujii, M. Hesse, & R. L. Lysak (Eds.), *Magnetospheric Current Systems*, AGU Geophysical Monograph (Vol. 118). Washington, DC: American Geophysical Union.

Kintner, P. M., & Seyler, C. E. (1985). The status of observations and theory of high latitude ionospheric and magnetocpheric plasma turbulence. *Space Science Reviews*, *41*, 91.

Knudsen, D. J., Burchill, J. K., Buchert, S. C., Eriksson, A. I., Gill, R., Wahlund, J.-E., et al. (2017). Thermal ion imagers and Langmuir probes in the Swarm electric field instruments. *Journal of Geophysical Research: Space Physics*, *122*, 2655–2673. https://doi.org/10.1002/2016JA022571

Kolmogorov, A. N. (1941a). Energy dissipation in locally isotropic turbulence. *Doklady Akademii Nauk SSSR*, *32*(1), 19–21.

Kolmogorov, A. N. (1941b). Local structure of turbulence in an incompressible fluid at very high Reynolds numbers. *Doklady Akademii Nauk SSSR*, *30*, 301.

Kolmogorov, A. N. (1962). A refinement of previous hypotheses concerning the local structure of turbulence in a viscous incompressible fluid at high Reynolds number. *Journal of Fluid Mechanics*, *13*, 82.

Korth, H., Anderson, B. J., & Waters, C. L. (2010). Statistical analysis of the dependence of large-scale Birkeland currents on solar wind parameters. *Annals of Geophysics*, *28*, 515–530. https://doi.org/10.5194/angeo-28-515-2010

Lepreti, F., et al. (2009). Yaglom law for electrostatic turbulence in laboratory magnetized plasmas. *Europhysics Letters*, *86*, 25,001. https://doi.org/10.1209/0295-5075/86/25001

Lühr, H., Huang, T., Wing, S., Kervalishvili, G., Rauberg, J., & Korth, H. (2016). Filamentary field-aligned currents at the polar cap region during northward interplanetary magnetic field derived with the Swarm constellation. *Annals of Geophysics*, *34*, 901–915. https://doi.org/10.5194/angeo-34-901-2016

Lühr, H., Warnecke, J., Zanetti, L. J., Lundquist, P. A., & Hughes, T. J. (1994). Fine structure of field-aligned current sheets deduced from spacecraft and ground-based observations: Initial Freja results. *Geophysical Research Letters*, *21*, 1883.

Lui, A. T. Y., Liou, K., Newell, P. T., Brittnacher, M. J., & Parks, G. K. (1998). Plasma and magnetic flux transport associated with auroral breakups. *Geophysical Research Letters*, *25*, 4059.

Mandelbrot, B. B., Fisher, A. J., & Calvet, L. E. (1997). A multifractal model of assets returns. Cowles Foundation discussion paper no. 1164.

Meneveau, C., & Sreenivasan, K. R. (1987). Simple multifractal cascade for fully developed turbulence. *Physical Review Letters*, *59*, 1424–1427.

Neubert, T., & Christiansen, F. (2003). Small-scale, field-aligned currents at the top-side ionosphere. *Geophysical Research Letters*, *30*(19), 2010. https://doi.org/10.1029/2003GL017808

Olsen, N. (1996). A new tool for determining ionospheric currents from magnetic satellite data. *Geophysical Research Letters*, *23*, 3635. https://doi.org/10.1029/96GL02896

Papitashvili, V. O., Christiansen, F., & Neubert, T. (2001). Field-aligned currents during IMF 0. *Geophysical Research Letters*, *28*, 3055–3058.

Papitashvili, V. O., & Rich, F. J. (2002). High-latitude ionospheric convection models derived from Defense Meteorological Satellite Program ion drift observations and parameterized by the interplanetary magnetic field strength and direction. *Journal of Geophysical Research*, *107*, 1198. https://doi.org/10.1029/2001JA000264

Pokhotelov, O. A., Pilipenko, V. A., Fedorov, E. N., Stenflo, L., & Shukla, P. K. (1994). Induced electromagnetic turbulence in the ionosphere and the magnetosphere. *Physica Scripta*, *50*, 600.

Ritter, P., Lühr, H., & Rauberg, J. (2013). Determining field-aligned currents with the Swarm constellation mission. *Earth Planets Space*, *65*, 1285–1294. https://doi.org/10.5047/eps.2013.09.006

Rother, M., Schlegel, K., & Lühr, H. (2007). CHAMP Observation of intense kilometer-scale field-aligned currents, evidence for an ionospheric alfvén resonator. *Annals of Geophysics*, *25*, 16031615. https://doi.org/10.5194/angeo-25-1603-2007

Sofko, G. J., Greenwald, R., & Bristow, W. (1995). Direct determination of large-scale magnetospheric field-aligned currents with superDARN. *Geophysical Research Letters*, *22*, 2041–2044.

Spicher, A., Miloch, W. J., Clausen, L. B. N., & Moen, J. I. (2015). Plasma turbulence and coherent structures in the polar cap observed by the ICI-2 sounding rocket. *Journal of Geophysical Research: Space Physics*, *120*, 10,959–10,978. https://doi.org/10.1002/2015JA021634

Stasiewicz, K., & Potemra, T. (1998). Multiscale current structures observed by Freja. *Journal of Geophysical Research*, *103*, 4315.

Tam Sunny, W. Y., Chang, T., Kintner, P. M., & Klatt, E. (2005). Intermittency analyses on the SIERRA measurements of the electric field fluctuations in the auroral zone. *Geophysical Research Letters*, *32*, L05109. https://doi.org/10.1029/2004GL021445

Tam Sunny, W. Y., Chang, T., Kintner, P. M., & Klatt, E. (2010). ROMA (Rank-Ordered Multifractal Analysis) For intermittent fluctuations with global crossover behavior. *Physical Review E*, *81*, 36414.

Wu, C. C., & Chang, T. (2000). 2D MHD simulation of the emergence and merging of coherent structures. *Geophysical Research Letters*, *27*, 863.

Wu, C. C., & Chang, T. (2001). Further study of the dynamics of two-dimensional MHD coherent structures large scale simulation. *Journal of Atmospheric and Solar-Terrestrial Physics*, *63*, 1447.

Zmuda, A. J., Martin, J. H., & Heuring, F. T. (1966). Transverse hydromagnetic disturbances at 1100 km in the auroral region. *Journal of Geophysical Research*, *71*, 5033–5045.